Cerebral Cortex, August 2018;28: 2699–2710

doi: 10.1093/cercor/bhx148
Advance Access Publication Date: 15 June 2017
Original Article

ORIGINAL ARTICLE

Fine Subdivisions of the Semantic Network Supporting Social and Sensory–Motor Semantic Processing

Nan Lin[1,2], Xiaoying Wang[3], Yangwen Xu[3], Xiaosha Wang[3], Huimin Hua[1,2], Ying Zhao[4] and Xingshan Li[1,2]

[1]CAS Key Laboratory of Behavioral Science, Institute of Psychology, Beijing 100101, China, [2]Department of Psychology, University of Chinese Academy of Sciences, Beijing 100049, China, [3]National Key Laboratory of Cognitive Neuroscience and Learning and IDG/McGovern Institute for Brain Research, Beijing Normal University, Beijing 100875, China and [4]Neuroscience and Aphasia Research Unit, Division of Neuroscience and Experimental Psychology, School of Biological Sciences, University of Manchester, Manchester M13 9PL, UK

Address correspondence to Nan Lin, CAS Key Laboratory of Behavioral Science, Institute of Psychology, Beijing 100101, China. Email: linn@psych.ac.cn

Abstract

Neuroimaging studies have consistently indicated that semantic processing involves a brain network consisting of multimodal cortical regions distributed in the frontal, parietal, and temporal lobes. However, little is known about how semantic information is organized and processed within the network. Some recent studies have indicated that sensory–motor semantic information modulates the activation of this network. Other studies have indicated that this network responds more to social semantic information than to other information. Using fMRI, we collectively investigated the brain activations evoked by social and sensory–motor semantic information by manipulating the sociality and imageability of verbs in a word comprehension task. We detected 2 subgroups of brain regions within the network showing sociality and imageability effects, respectively. The 2 subgroups of regions are distinct but overlap in bilateral angular gyri and adjacent middle temporal gyri. A follow-up analysis of resting-state functional connectivity showed that dissociation of the 2 subgroups of regions is partially associated with their intrinsic functional connectivity differences. Additionally, an interaction effect of sociality and imageability was observed in the left anterior temporal lobe. Our findings indicate that the multimodal cortical semantic network has fine subdivisions that process and integrate social and sensory–motor semantic information.

Key words: fMRI, imageability, social concept, theory of mind, verb

Introduction

Neuroimaging studies have indicated that a brain network consisting of multimodal cortical areas is involved in semantic processing (Ferstl et al. 2008; Binder et al. 2009). The network includes but is not limited to the temporoparietal junction (TPJ), angular gyrus (AG), middle temporal gyrus (MTG), ventromedial temporal cortex (VMTC), posterior cingulate gyrus (PC) and adjacent precuneus, dorsomedial prefrontal cortex (DMPFC), ventromedial prefrontal cortex, and inferior frontal gyrus (IFG). This multimodal cortical semantic network is activated in various domains of cognitive processes requiring semantic retrieval, such as language comprehension, theory of mind (ToM), autobiographical memory, and prospection (Binder et al. 2009; Spreng et al. 2009; Mar 2011), and is often referred to as a "general semantic network" (Binder et al. 2009). However, increasing evidence indicates that the multimodal cortical semantic network organizes semantic information along particular dimensions and may have fine divisions to process different types of semantic information.

One line of studies has indicated that sensory–motor semantic information modulates the activation of the multimodal cortical

semantic network. Brain activation evoked by sensory–motor semantic information was initially observed within sensory and motor systems (Martin et al. 1995). Early evidence indicating that sensory–motor semantic information also modulates the activation of multimodal cortical semantic network came from the observation that several areas of the network, including the superior frontal gyrus (SFG) and adjacent middle frontal gyrus (MFG), PC/precuneus, AG, and VMTC, respond more to high-imageability nouns, which are assumed to be rich in sensory–motor information, than to low-imageability nouns (Jessen et al. 2000; Binder et al. 2005; Sabsevitz et al. 2005; Fliessbach et al. 2006; Graves et al. 2010). A recent study (Fernandino et al. 2016a) provided more direct and detailed evidence about how sensory–motor semantic information is processed within the multimodal cortical semantic network. The authors collected the brain activation patterns, as well as salience ratings in terms of 5 sensory–motor semantic attributes, that is, color, shape, visual motion, sound, and manipulation, for a set of 900 English nouns. It was found that the ratings of the sensory–motor semantic attributes parametrically modulated brain activations in the multimodal cortical semantic network in a hierarchical fashion: the peripheral regions of the network, which have more direct connections to the sensory–motor systems, were sensitive to one or some of the attributes; the core regions, whose distributions are largely consistent with those showing imageability effect in previous studies, were associated with all of the 5 attributes. In addition, 2 follow-up studies further showed that the ratings of the 5 sensory–motor attributes could be used to predict brain activations evoked by individual concepts, even when the analysis was restricted to the multimodal cortical semantic network (Fernandino et al. 2015, 2016b). Based on these findings, Fernandino et al. (2016a, 2016b) proposed that the multimodal cortical semantic network represents semantic information as multimodal combinations of sensory and motor representations.

Another line of studies has indicated that social semantic information modulates the activation of the multimodal cortical semantic network. A group of regions within the multimodal cortical semantic network, including the TPJ/AG, DMPFC, PC/precuneus, and anterior superior temporal sulcus (ASTS), have been found to be involved in social cognition tasks, especially those requiring thinking of other people's thought (Gallagher et al. 2000; Saxe and Kanwisher 2003; Mar 2011; Schurz et al. 2014). These regions are often collectively referred to as the ToM network. Several studies of word comprehension have found that words describing human characteristics and behaviors evoke stronger activation in the ToM network than those denoting nonhuman concepts do (Mitchell et al. 2002; Zahn et al. 2007; Contreras et al. 2012; Binney et al. 2016). Recently, Lin et al. (2015) further demonstrated that the ToM network is more sensitive to semantic attributes associated with social interactions between people than to non-social human attributes. In that study, Lin et al. (2015) compared brain activations evoked by verbs that refer to social actions of humans (e.g., "embrace"), private actions of humans (e.g., "walk"), and nonhuman events (e.g., "burn") in a semantic relatedness judgment task. It was found that all classic regions of the ToM network showed much stronger activations to social action verbs than the other 2 types of verbs. Therefore, Lin et al. (2015) proposed that the ToM network supports processing of semantic information associated with social interactions.

According to the above 2 lines of studies, the brain regions supporting sensory–motor semantic information and those supporting social semantic information may overlap with each other, especially in the AG and PC/precuneus. However, because the previous studies have not simultaneously considered sensory–motor and sociality effects, the observation of one effect may actually reflect the confounding of the other; or the 2 effects may counteract or override each other, leading to inconsistent results. Confusion between sensory–motor and sociality effects may explain the inconsistent findings about the verb imageability effect in the AG and PC/precuneus. Although the imageability effect in the AG and PC/precuneus was frequently observed in studies using nouns as stimuli (Jessen et al. 2000; Binder et al. 2005; Sabsevitz et al. 2005; Fliessbach et al. 2006; Graves et al. 2010), most studies using verbs as stimuli did not find such effect (Perani et al. 1999; Grossman et al. 2002; Raposo et al. 2009; Rodriguez-Ferreiro et al. 2011) or only partially replicated it (Bedny and Thompson-Schill 2006; van Dam et al. 2010). Some studies even found a reverse imageability effect (high-imageability verb < low-imageability verb) in the AG and/or PC/precuneus (Tettamanti et al. 2005; Pexman et al. 2007). A recent study (Spunt et al. 2016) focused on the level of conceptual abstraction (LOA) of verb phrases, which has a high correlation with imageability ($r = -0.97$ as reported in Spunt et al. (2016)). The study found that the high LOA (low-imageability) phrases (e.g., "contact a friend") evoked stronger activations than low LOA (high-imageability) phases (e.g., "make a phone call") in all classic regions of the ToM network, including the TPJ/AG and PC/precuneus. We translated the stimuli used by Spunt et al. (2016) into Chinese and asked 16 participants (with 13 females) to rate them on a 5-point scale considering how often these stimuli involve interactions between people (5 = "always," 4 = "typically but not necessarily," 3 = "sometimes," 2 = "rarely," and 1 = "never"). The sociality ratings of the stimuli showed a strong correlation ($r = 0.53$) with the LOA ratings provided by Spunt et al. (2016), indicating that there might be confusion between LOA/imageability and sociality effects. Therefore, to obtain reliable effects of sociality and imageability, the 2 effects need to be re-examined by controlling for each other.

Another question is where and how the brain regions supporting sensory–motor semantics and those supporting social semantics "communicate" with each other. Based on existing evidence, although these 2 sets of brain regions may overlap with each other in the AG and PC/precuneus, they should be at least partially distinct from each other (Binder et al. 2016; Huth et al. 2016). Therefore, the multimodal cortical semantic network contains at least 2 subsystems: one processes sensory–motor semantic information and the other processes social semantic information. These 2 subsystems should have some connectors to "communicate" with each other, allowing the semantic network to integrate and unify sensory–motor and social semantics. Based on existing evidence from task fMRI studies, the AG and PC/precuneus, where both types of effects have been observed to date (Binder et al. 2005; Sabsevitz et al. 2005; Graves et al. 2010; Lin et al. 2015), could be the candidate regions. The findings of a recent study (Xu et al. 2016) provide another clue to this question. The study found that, according to resting-state functional connectivity (RSFC), the multimodal semantic network can be divided into 3 subnetworks: 2 of them largely correspond to the brain regions showing imageability and sociality effects, with 1 containing AG, PC/precuneus, VMTC, and SFG/MFG and the other containing TPJ/AG, ASTS, and DMPFC. The connector nodes of these 2 subnetworks were found in the AG, ASTS, and SFG. Thus, the 2 lines of evidence collectively indicated AG as the candidate region connecting the sensory–motor and social semantic subsystems.

To tease apart sociality and imageability effects and to explore the connectors between the sensory–motor and social

semantic subsystems, the brain activations evoked by social and sensory–motor semantic information need to be collectively examined in a single experiment. To this end, we conducted a functional magnetic resonance imaging (fMRI) study in which we manipulated the sociality and imageability of verbs and investigated how these 2 factors modulate brain activation in a semantic relatedness judgment task.

Materials and Methods

Participants

A total of 19 healthy undergraduate and graduate students (10 females) participated in the fMRI experiment. The average age of the participants was 23.5 years (SD = 2.7 years). All participants were right-handed and were native Chinese speakers. The participants neither suffered from psychiatric or neurological disorders nor had ever sustained head injury. Prior to the experiment, each participant read and signed an informed consent form issued by the Institutional Review Board of the Magnetic Resonance Imaging Research Center, the Institute of Psychology of the Chinese Academy of Science.

Procedure

The main experiment contained 4 conditions, namely, the high-sociality and high-imageability condition (HSHI; e.g., "embrace"), the high-sociality and low-imageability condition (HSLI; e.g., "trust"), the low-sociality and high-imageability condition (LSHI; e.g., "walk"), and the low-sociality and low-imageability condition (LSLI; e.g., "infer"). Two prior rating experiments were conducted with additional participants to obtain the sociality and imageability ratings of 370 Chinese verbs. In the sociality rating experiment, 16 participants (10 females) were asked to classify verbs on a 5-point scale according to how often an event that a verb refers to involves interaction between people (5 = "always," 4 = "typically but not necessarily," 3 = "sometimes," 2 = "rarely," and 1 = "never"). In the imageability rating experiment, another group of 16 participants (11 females) were asked to rate on a 5-point scale the extent to which the meaning of a verb brought to mind an image (5 = "very high" and 1 = "very low"). In both rating experiments, inter-rater reliability (Shrout and Fleiss 1979) was high (sociality rating: ICC [2, 16] = 0.953; imageability rating: ICC [2, 16] = 0.966).

On the basis of participant ratings, 240 verbs were then selected as materials (60 per condition). The ratings of the 4 conditions are presented in Table 1. The HSHI, HSLI, LSHI, and LSLI conditions scored 4.28 (SD = 0.54), 4.19 (SD = 0.35), 2.14 (SD = 0.51), and 2.22 (SD = 0.38) points of sociality, respectively. The sociality ratings were significantly different between the high-sociality and low-sociality conditions (*t*s [118] > 22; *P*s < 0.001) and were matched between the HSHI and HSLI conditions and between the LSHI and LSLI conditions (*t*s [118] < 1). The HSHI, HSLI, LSHI, and LSLI conditions scored 4.12 (SD = 0.44), 1.93 (SD = 0.42), 4.16 (SD = 0.46), and 1.86 (SD = 0.38) points of imageability, respectively. The imageability ratings were significantly different between the high-imageability and low-imageability conditions (*t*s [118] > 27; *P*s < 0.001) and were matched between the HSHI and LSHI conditions and between the HSLI and LSLI conditions (*t*s [118] < 1). All of the 240 verbs are 2-character and disyllabic Chinese words. The word frequency obtained from the Language Corpus System of Modern Chinese Studies (Sun et al. 1997) was also matched between conditions (mean frequency count per million [SD]: HSHI = 9.7 [12.2]; HSLI = 10.8 [15.4]; LSHI = 11.5 [13.9]; and LSLI = 10.9 [13.8]; *t*s [118] < 1). Considering that semantic ambiguity of a word's meaning is an important factor affecting lexical process (Millis and Button 1989; Azuma and Van Orden 1997; Rodd et al. 2002; Shen and Li 2016), we inspected the numbers of homonymous and polysemous words in our materials on the basis of the Contemporary Chinese Dictionary (Chinese Academy of Sciences 2005). The materials contain no homonymous words and 49 polysemous words. The proportions of polysemous words were low and similar across conditions (HSHI = 15/60; HSLI = 10/60; LSHI = 12/60; and LSLI = 12/60; χ^2s < 1.264, *P*s > 0.261). Therefore, the semantic ambiguity effect should be small and similar across conditions and thus should not confound our results. The 240 verbs were then used to constitute 240 different verb pairs. Each verb appeared twice in the experiment and was paired with different verbs. The paired verbs were always from the same condition.

The main fMRI experiment employed an event-related design with 4 runs of 6 min 10 s each. Each run included 15 trials for each condition. The first 10 s of each run was a fixation. We used a semantic relatedness judgment task in which participants saw a pair of verbs and were asked to indicate whether these verbs were strongly related in meaning by pressing buttons. In each trial, the verbs appeared for 3 s, followed by a jitter fixation of at least 1 s. The order of trials and the length of jitter fixations were optimized using optseq software (http://surfer.nmr.mgh.harvard.edu/optseq/) and were counterbalanced across runs and participants.

In addition to the main fMRI experiment, a ToM localizer experiment was also conducted to investigate whether the brain regions showing sociality effect overlap with the classic ToM network. The task was adapted from the publicly available false-belief localizer (Dodell-Feder et al. 2011). It included 10 belief stories and 10 photo stories, all of which described an outdated representation (a false belief or a false photo/picture). We translated the stories into Chinese and made a few modifications to adapt to the cultural differences (e.g., changing the English names into Chinese names) and to match the length and sentence numbers between the 2 conditions. Each story was presented for 10 s, followed by a true/false question

Table 1. Lexical-semantic variables for each condition

Condition	Example	Sociality	Imageability	Word length	Syllable length	Word frequency (per million)	Proportion of polysemous words
HSHI	拥抱 (embrace)	4.28 ± 0.54	4.12 ± 0.44	2 ± 0	2 ± 0	9.7 ± 12.2	15/60
HSLI	信赖 (trust)	4.19 ± 0.35	1.93 ± 0.42	2 ± 0	2 ± 0	10.8 ± 15.4	10/60
LSHI	行走 (walk)	2.14 ± 0.51	4.16 ± 0.46	2 ± 0	2 ± 0	11.5 ± 13.9	12/60
LSLI	推断 (infer)	2.22 ± 0.38	1.86 ± 0.38	2 ± 0	2 ± 0	10.9 ± 13.8	12/60

Note. The sociality, imageability, word length, syllable length, and word frequency were presented in form of mean ± standard deviation.

(presented for 4 s) and a 12 s fixation. The stories were presented sentence by sentence. Within a story, the presentation time of each sentence was linearly dependent to its length. All stories were presented within a single run lasting 8 min 50 s, with the first 10 s of the run being a fixation.

Data Acquisition and Preprocessing

Structural and functional data were collected with a GE Discovery MR750 3 T scanner at the Magnetic Resonance Imaging Research Center, the Institute of Psychology of the Chinese Academy of Science. T1-weighted structural images were collected in 176 sagittal slices with 1.0 mm isotropic voxels. For the tasks, functional blood-oxygenation-level-dependent data were obtained in 3.0 mm isotropic voxels (TR = 2 s; TE = 30 ms) in 42 near-axial slices. Before the tasks were performed, resting-state fMRI data were collected for all but one participants, which were obtained in 3.4 mm × 3.4 mm × 4 mm voxels (TR = 2 s; TE = 30 ms) in 35 axial slices.

The fMRI data were preprocessed using the Statistical Parametric Mapping software (SPM8; http://www.fil.ion.ucl.ac.uk/spm/) and the advanced edition of DPARSF V2.3 (Yan and Zang 2010). For both the main and localizer tasks, the first 5 volumes (10 s) of each functional run were discarded for signal equilibrium. Slicing timing and 3-D head motion correction were then performed, and a mean functional image was obtained for each participant. The structural image of each participant was coregistered to the mean functional image and subsequently segmented using the unified segmentation VBM module (Ashburner and Friston 2005) implemented in DPARSFA. The parameters obtained during segmentation were used to normalize the functional images of each participant onto the Montreal Neurological Institute space. The functional images were then spatially smoothed using a 6 mm FWHM Gaussian kernel.

For preprocessing of resting-state fMRI data, the first 10 volumes (20 s) were discarded, followed by steps that were similar to those of the task fMRI data, except that the effects of nuisance variables, including 6 rigid head motion parameters, white matter signal, and cerebrospinal fluid signal, were regressed from the functional images before spatial normalization. The data of one participant was discarded because of excessive head movement (>2.0 mm or 2.0° in any direction). After those steps, linear trends were removed and the images were 0.01–0.1 Hz band-pass filtered to reduce the effects of low-frequency drifts and high-frequency noise.

Data Analysis

Statistical analyses on the task fMRI data were conducted according to 2-level, mixed-effects models implemented in SPM8. For the main task, at the first level, a general linear model was applied to explore the fixed effect of each participant. The 4 conditions (HSHI, HSLI, LSHI, and LSLI) were set as covariates of interest and the onset of each trial was modeled as an event with duration of 0 s. Six head motion parameters, which were obtained by head motion correction, were included as nuisance regressors. Considering that the effect of RT has been found to be a strong confounding factor in cognitive neuroimaging studies (Yarkoni et al. 2009), the effect of RT was also included as a nuisance covariate, which was constructed by modulating the amplitude of the predicted neural response for each trial of interest by the demeaned RT value. A supplemental analysis in which the effect of RT was not removed was also conducted for comprehensive inspection. Time series data were subjected to a high-pass filter (128 Hz). After the estimation of model parameters, participant-specific statistical maps were generated and entered into a second-level, random-effects analysis, in which a flexible factorial design was applied to accommodate a 2 × 2 within-subject design. The main effects, that is, sociality and imageability effects, and their interaction were examined. A whole-brain conjunction analysis was further conducted to locate regions sensitive to both of the 2 main effects (Nichols et al. 2005).

For the localizer experiment, at the first level, the 2 conditions ("belief" and "photo") were set as covariates of interest, and each trial was modeled as a block with a boxcar lasting 14 s from the onset of the story presentation to the end of the question presentation. Six head motion parameters were included as nuisance regressors and time series data were subjected to a high-pass filter (128 Hz). After the model parameters were estimated, a contrast between the 2 conditions ("belief" and "photo") was generated and computed for every participant. At the second level, the contrast image of each participant ("belief" vs. "photo") was entered into a one-sample t test.

For both the main and localizer tasks, the false positive rate was controlled at $\alpha < 0.05$ (with the individual voxel threshold probability setting of $P < 0.001$) using a Monte Carlo simulation program (which is similar to the AlphaSim in AFNI) implemented in DPABI V2.1 (Yan et al. 2016). Considering recent concerns regarding clusterwise multiple comparison correction (Eklund et al. 2016), we further inspected the significance of the peak voxels of the emerged clusters by using voxelwise FWE correction implemented in SPM8, which served as a supplementary and conservative method of multiple comparison correction. The results were shown using the Brainnet Viewer software (Xia et al. 2013).

After identifying the brain regions showing sociality and imageability effects, we performed 3 follow-up analyses to investigate their network properties. In the first analysis, we examined whether the brain regions showing sociality effect in the main task overlapped with the classic ToM network. To this end, we defined the results ("belief" > "photo") of the ToM localizer experiment as a mask. Then, for each cluster showing sociality effect in the main experiment, we calculated the proportion of its voxels that overlapped with the ToM mask. We expected that, if the brain regions showing sociality effect corresponded to the classic ToM network, then they should highly overlap with the ToM mask.

In the second analysis, we investigated whether the dissociation between the 2 groups of brain regions follows the divides of the 7 intrinsic large-scale brain networks identified by Yeo et al. (2011). The 7 intrinsic large-scale brain networks were obtained based on 1000 healthy young participants. These intrinsic large-scale brain networks were proposed to support different basic cognitive processes. Therefore, if the dissociation between sociality and imageability effects follows the divides of these networks, it would indicate that the 2 effects may be associated with different basic cognitive processes. For example, we observed sociality and imageability effects in the AG/MTG, with the sociality effect being anterior to the imageability effect. If the dissociation of the 2 effects follows the divides between the ventral-attention network and the default-mode network in this region, then the 2 effects may be associated with bottom-up attention and episodic memory, respectively (Hutchinson et al. 2009, 2014; Uddin et al. 2010; Mars et al. 2011; Nelson et al. 2012). To examine this possibility, for each cluster showing sociality or imageability effect, we calculated the numbers of voxels that overlapped with the templates of the 7 intrinsic brain networks

(Yeo et al. 2011). Our expectation was that, if the dissociation between the 2 groups of brain regions is associated with the functional differences between the 7 intrinsic brain networks, then they should have highly distinct distributions in these networks.

In the third analysis, we defined the clusters showing sociality and imageability effects as regions of interest (ROIs) and investigated whether the functional association and dissociation between the ROIs are associated with the RSFC between them. The RSFC analysis was conducted using the Resting-state fMRI Data Analysis Toolkit (REST version 1.8; http://www.restfmri.net) (Song et al. 2011). For each participant, the mean time series of each ROI was calculated and correlated with each other. For visualization purposes, we created a matrix to show the average RSFC between each pair of ROIs across subjects. The correlation coefficient between each pair of ROIs was Fisher-transformed and averaged across subjects (the Fisher transform decreases the bias in averaging; Silver and Dunlap 1987) and was then inverse Fisher transformed and presented in the matrix.

We performed 2 sets of comparisons to examine the network properties of these ROIs. The statistical analyses were performed by using within-subject *t*-tests, in which the correlation coefficients were Fisher-transformed to improve normality. In the first set of comparisons, we examined whether the dissociation between the 2 groups of ROIs (sociality-ROIs and imageability-ROIs) is associated with their intrinsic functional connectivity properties. To this end, we compared the average RSFC (Fisher-transformed correlation coefficient) within each group of ROIs with the average RSFC across the 2 groups of ROIs. Our expectation was that, if the 2 groups of ROIs correspond to 2 intrinsic brain networks, then the average RSFC within each group of ROIs should be stronger than the average RSFC across the 2 groups.

Because the regions showing sociality effect and the regions showing imageability effect were adjacent and partially overlapped each other in the AG/MTG and PC/precuneus, we conducted a second set of comparisons to examine whether the functional dissociation between the adjacent areas in the AG/MTG and PC/precuneus is associated with their intrinsic functional connectivity to the other brain regions. To this end, the ROIs were classified into 4 groups: the sociality- and imageability-ROIs that partially overlapped each other were classified as "connector sociality-ROIs" and "connector imageability-ROIs"; the other sociality- and imageability-ROIs were classified as "provincial sociality-ROIs" and "provincial imageability-ROIs." We expected that, if the dissociation between the 2 groups of connector ROIs is associated with their intrinsic functional connectivity to the provincial ROIs, then the provincial sociality-ROIs should show stronger RSFC to the connector sociality-ROIs than to connector imageability-ROIs and the provincial imageability-ROIs should show stronger RSFC to connector imageability-ROIs than to connector sociality-ROIs.

Results

Behavioral Results

The participants judged the semantic relatedness (strong/weak) of pairs of words by pressing buttons. The mean RTs of the HSHI, HSLI, LSHI, and LSLI conditions were 1488 ms (SD = 205 ms), 1587 ms (SD = 222 ms), 1442 ms (SD = 205 ms), and 1568 ms (SD = 219 ms), respectively. The main effects of sociality and imageability on RTs were statistically significant (sociality: $F_{1,19} = 5.41$, $P = 0.033$, high > low; imageability: $F_{1,19} = 68.16$, $P < 0.001$, high < low), but the "sociality × imageability" interaction was not ($F_{1,19} < 1$). Meanwhile, the mean semantic relatedness ratings (strong = 1/weak = 0) of the HSHI, HSLI, LSHI, and LSLI conditions were 0.55 (SD = 0.09), 0.52 (SD = 0.11), 0.57 (SD = 0.09), and 0.50 (SD = 0.09), respectively. The main effects of imageability and the "sociality × imageability" interaction on relatedness were significant (imageability: $F_{1,19} = 9.25$, $P = 0.007$, high > low; interaction: $F_{1,19} = 6.78$, $P = 0.019$), but the main effect of sociality was not ($F_{1,19} < 1$).

Task-fMRI Results

The results of the main analysis of the fMRI data are shown in Table 2. Bilateral ASTS, DMPFC, PC/precuneus, AG, MTG and right superior temporal gyrus (STG) showed the sociality effect (high-sociality verb > low-sociality verb) and no region showed a reverse pattern (Fig. 1*A*). Bilateral PC/precuneus, VMTC, SFG/MFG, IFG, AG, middle occipital gyrus (MOG), MTG, inferior temporal gyrus (ITG), and left middle cingulate gyrus showed the imageability effect (high-imageability verb > low-imageability verb) and no region showed the reverse effect (high-imageability verb < low-imageability verb) (Fig. 1*B*). Interaction of sociality and imageability was observed in the left ASTS (Fig. 1*C*). Inspection of the response pattern of this region (bar plots in Fig. 1*C*) showed that the activation level of the brain region for the HSHI verbs was high (beta = 4.99) and the activation level for the other 3 types of verbs was low and approximately the same (HSLI: beta = 1.71; LSHI: beta = 1.42; LSLI: beta = 1.59). For all except one cluster (the cluster showing imageability effect in left middle cingulate gyrus) reported above, the significance of their peak voxels survived the voxelwise FWE correction, indicating that the observed activations were reliable.

The distributions of the 2 main effects and their overlaps are shown in the top panel of Figure 1*D*. The conjunction analysis of the 2 main effects (high-sociality verb > low-sociality verb; high-imageability verb > low-imageability verb) found 2 significant clusters in bilateral AG/MTG (cluster sizes: 122 voxels in the left AG/MTG, 109 voxels in the right AG/MTG). A small cluster (cluster sizes: 19 voxels) in the left PC/precuneus also showed the conjunction effect but did not reach the cluster-size threshold. Considering that the group-level conjunction effect may result from individual differences in distributions of the sociality and imageability effects despite no conjunction effect in any single participant, we further inspected the conjunction effect at the individual level. A lenient threshold (uncorrected individual voxel threshold $P < 0.01$, cluster size ≥ 10 voxels) was chosen to explore how many participants had the trend toward showing the conjunction effect in bilateral AG/MTG. The conjunction effect was observed in about half of our participants (11/19 participants in the left AG/MTG and in 7/19 participants in the right AG/MTG; see the middle and bottom panels of Fig. 1*D* for the results of 2 representative participants), indicating that the group-level conjunction effect should not merely be a reflection of individual differences in the distributions of the 2 single effects. However, the fact that the conjunction effect was observed only in half of the participants also indicated that there might be considerable individual variability in the strength or existence of the conjunction effect, which must be considered with caution and should be investigated in future studies.

The results of supplementary analysis that did not include RT as a nuisance covariate are highly consistent with those of the main analysis, except that additional reverse imageability

Table 2. Results of the task fMRI data analysis

Contrast	Anatomical region of the peak voxel	Cluster size (voxels)	MNI coordinates of peak voxel (x, y, z)			Peak *t* value
Main effect of sociality						
HS > LS	Left temporal pole	197	−42	12	−36	7.91
	Left superior frontal gyrus	388	−9	51	36	6.71
	Left middle temporal gyrus	336	−48	−60	21	6.29
	Right temporal pole	162	45	21	−33	5.84
	Right superior temporal gyrus	213	51	−57	21	5.67
	Left posterior cingulate gyrus	100	−3	−51	21	5.55
HS < LS	None					
Main effect of imageability						
HI > LI	Left parahippocampal gyrus	312	−30	−30	−18	10.36
	Left middle occipital gyrus	404	−42	−72	24	9.80
	Left precuneus	400	−6	−54	12	8.84
	Left inferior frontal gyrus (pars orbitalis)	81	−30	30	−12	7.77
	Left inferior temporal gyrus	84	−57	−51	−6	7.54
	Right angular gyrus	295	45	−63	24	7.43
	Right parahippocampal gyrus	161	33	−30	−18	6.97
	Right inferior frontal gyrus (pars orbitalis)	64	33	33	−12	6.46
	Left middle frontal gyrus	217	−24	18	51	6.02
	Right middle temporal gyrus	69	60	−48	−6	5.47
	Right superior frontal gyrus	85	24	24	51	5.44
	Left middle cingulate gyrus	56	−6	−33	48	4.30
HI < LI	None					
"Sociality × imageability" interaction						
HSHI + LSLI > HSLI + LSHI	Left middle temporal gyrus	56	−54	−3	−15	5.82
HSHI + LSLI < HSLI + LSHI	None					

Note. The labels of "HS," "LS," "HI," and "LI" represent high-sociality, low-sociality, high-imageability, and low-imageability, respectively. The false positive rate was controlled at $\alpha < 0.05$ (with the individual voxel threshold probability setting of $P < 0.001$) using a Monte Carlo simulation program implemented in DPABI V2.1. The anatomical regions were identified by using the automated anatomical labeling template (Tzourio-Mazoyer et al. 2002).

effect (high-imageability verb < low-imageability verb) was observed in the left premotor cortex, IFG, and anterior temporal lobe (ATL) (see Supplementary Fig. 1). Such an effect could also be observed in the results of the main analysis if an uncorrected threshold ($P < 0.001$, cluster size = 10 voxels) was used. The reverse imageability effect is consistent with findings in the literature (Binder et al. 2009; Wang et al. 2010) but is beyond the scope of the present study, so it is not discussed further.

Follow-up Analyses: Exploring the Network Properties of the Brain Regions Showing Sociality and Imageability Effects

Do the Brain Regions Showing Sociality Effect Overlap with the Classic ToM Network?

The classic ToM network was defined by using a false-belief localizer (Dodell-Feder et al. 2011). During the task, participants answered the true/false questions following belief and photo stories by pressing buttons. No significant difference in RT or accuracy was found between conditions (mean RT [SD]: belief = 2764 ms [725 ms]; photo = 2922 ms [652 ms]; $t[19] = 1.35$, $P = 0.116$; mean accuracy [SD]: belief = 86.8% [14.2%]; photo = 83.7% [11.6%]; $t[19] < 1$). The results of the localizer experiment are shown in Supplementary Table 1 and Supplementary Figure 2. The belief stories evoked stronger activation than the photo stories in all classic components of the ToM network and in bilateral MFG, IFG, caudate, and right occipital lobe. The photo stories evoked stronger activation than the belief stories in bilateral MFG.

The brain regions showing significant "belief > photo" effect were defined as a mask. For each cluster showing sociality effect in the main experiment, we calculated the proportion of its voxels that overlap with the mask. All clusters have their majority of voxels overlapping with the mask (left ASTS: 88%; right ASTS: 88%; DMPFC: 99%; PC/precuneus: 89%; left AG/MTG: 97%; right AG/MTG/STG: 87%), indicating that these clusters largely correspond to classical ToM network.

Does the Dissociation Between Sociality and Imageability Clusters Follow the Divides Between the 7 Intrinsic Large-Scale Brain Networks?

For each cluster showing sociality or imageability effect in our main task, we calculated the numbers of voxels that overlap with the templates of the 7 intrinsic brain networks (Yeo et al. 2011). Following Yeo et al. (2011), the 7 networks were named as visual, somatomotor, dorsal attention, ventral attention, limbic, frontoparietal, and default mode networks, respectively. As shown in Table 3, all sociality clusters were mainly distributed in the default-mode network and their overlaps with the other networks were all small. The imageability clusters, although partially overlapped with the dorsal attention network, the frontoparietal network, and the visual network, were also mainly distributed in the default-mode network. Therefore, the dissociation between sociality and imageability clusters largely reflects functional heterogeneity in the default-mode network.

The ROI-Based RSFC Analysis

We conducted ROI-based RSFC analysis to further investigate whether the association and dissociation of the brain regions showing sociality and imageability effects are related to their intrinsic functional connectivity properties. As shown in Figure 2,

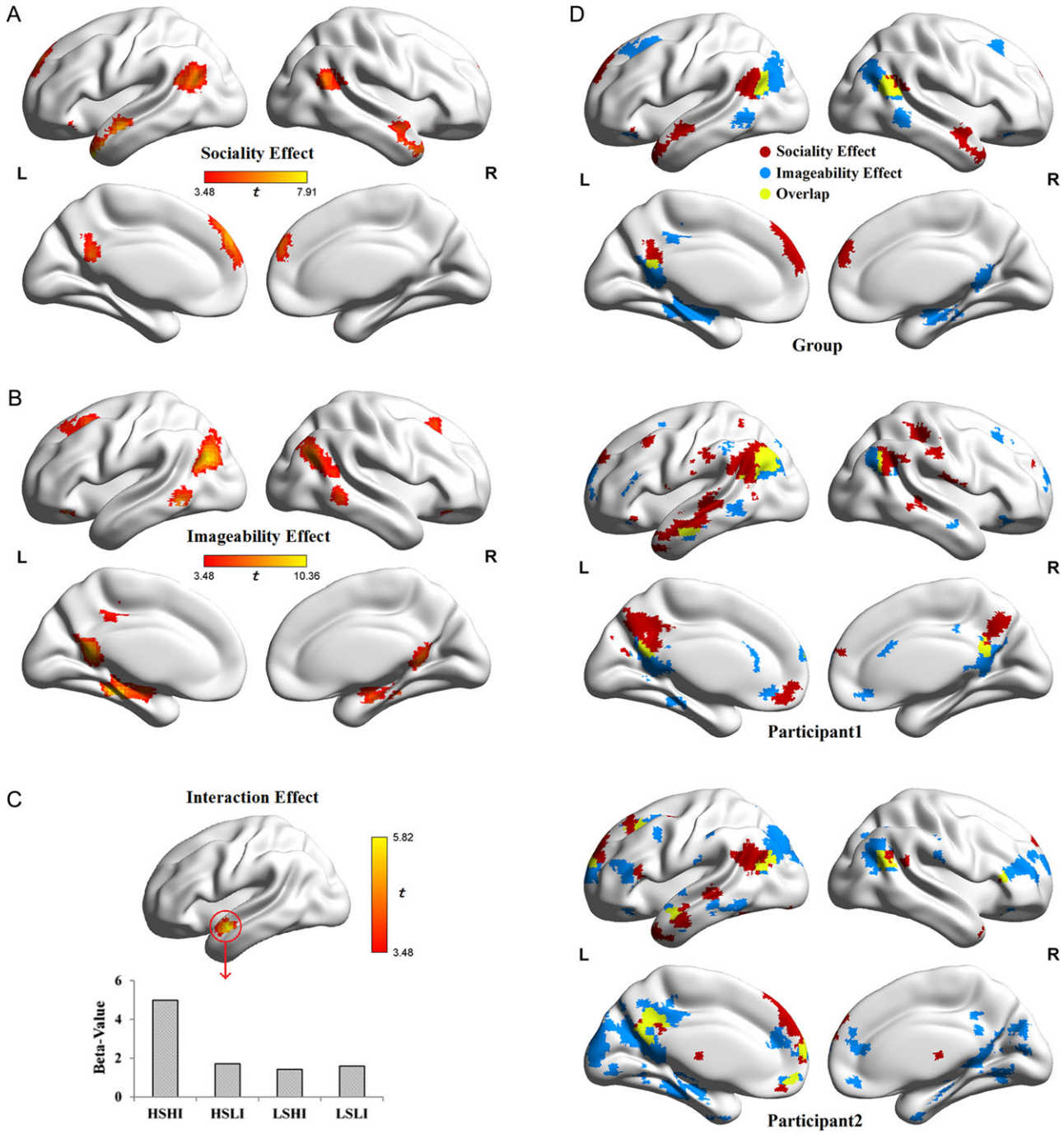

Figure 1. Results of the task analysis. (*A*) the main effect of sociality (warm color indicates stronger activation to high-sociality verbs than to low-sociality verbs), (*B*) the main effect of imageability (warm color indicates stronger activation to high-imageability verbs than to low-imageability verbs), (*C*) the interaction effect of sociality and imageability, and (*D*) the overlap and dissociation of the 2 main effects. The false positive rate was controlled at $\alpha < 0.05$ (with individual voxel threshold probability setting of $P < 0.001$) using a Monte Carlo simulation program implemented in DPABI V2.1.

all sociality-ROIs showed strong RSFC to each other. However, for the imageability-ROIs, strong RSFC was only observed between connector imageability-ROIs, between connector imageability-ROIs and some provincial ROIs, and between the provincial ROIs that were bihemispherically symmetric.

We further conducted 2 statistical comparisons to investigate the RSFC pattern across the ROIs. In the first set of comparisons, we compared the average RSFC within a group of ROIs (sociality or imageability) with the average RSFC across the 2 groups. We found that the average RSFC within the sociality-ROIs was significantly stronger than the average RSFC across the 2 groups (mean Fisher-transformed correlation [SD]: within sociality-ROIs = 0.71 [0.20]; across groups = 0.39 [0.11]; $t[16] = 10.76$, $P < 0.001$); however, there was no significant difference between the average RSFC within the imageability-ROI group and the average RSFC across the 2 groups (mean Fisher-transformed correlation [SD]: within imageability-ROIs = 0.37 [0.11]; across groups = 0.39 [0.11]; $t[16] = 1.52$, $P = 0.149$).

Table 3. The distributions of sociality and imageability clusters in the 7 intrinsic large-scale brain networks (Yeo et al. 2011)

Contrast	Anatomical region of the peak voxel of the cluster	The number of voxels overlapping with the 7 intrinsic brain networks						
		Visual	Somatomotor	Dorsal attention	Ventral attention	Limbic	Frontoparietal	Default
Main effect of sociality								
HS > LS	Left temporal pole	0	4	0	0	36	0	152
	Left superior frontal gyrus	0	0	0	0	0	0	337
	Left middle temporal gyrus	2	0	30	11	0	0	232
	Right temporal pole	0	8	0	0	26	0	126
	Right superior temporal gyrus	0	0	35	7	0	0	168
	Left posterior cingulate gyrus	0	0	0	0	0	0	90
	Total	*2*	*12*	*65*	*18*	*62*	*0*	*1105*
Main effect of imageability								
HI > LI	Left parahippocampal gyrus	47	0	6	0	1	0	43
	Left middle occipital gyrus	39	0	97	0	0	31	165
	Left precuneus	62	0	0	0	0	0	228
	Left inferior frontal gyrus (pars orbitalis)	0	0	0	4	12	18	23
	Left inferior temporal gyrus	0	0	27	1	0	31	6
	Right angular gyrus	0	0	75	0	0	6	162
	Right parahippocampal gyrus	35	0	0	0	8	0	0
	Right inferior frontal gyrus (pars orbitalis)	0	0	0	0	3	20	18
	Left middle frontal gyrus	0	0	2	0	0	51	147
	Right middle temporal gyrus	0	0	21	14	0	19	7
	Right superior frontal gyrus	0	0	0	0	0	24	57
	Left middle cingulate gyrus	0	8	0	16	0	9	23
	Total	*183*	*8*	*228*	*35*	*24*	*209*	*879*

Note. The labels of "HS," "LS," "HI," and "LI" represent high-sociality, low-sociality, high-imageability, and low-imageability, respectively. The anatomical regions were identified by using the automated anatomical labeling template (Tzourio-Mazoyer et al. 2002).

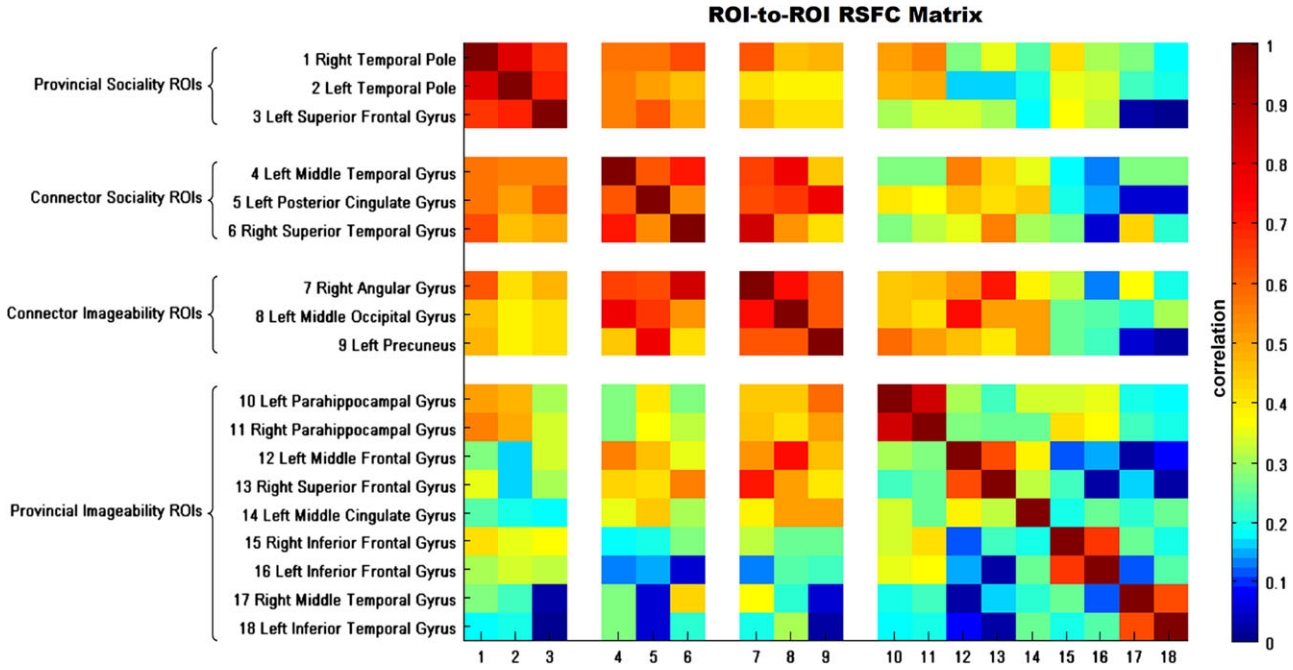

Figure 2. The matrix of ROI-to-ROI RSFC. The clusters showing sociality and imageability effects in the task-fMRI results were defined as ROIs. The ROIs were further classified into 4 groups: the sociality- and imageability-ROIs that partially overlapped each other were classified as "connector sociality-ROIs" and "connector imageability-ROIs"; the other sociality- and imageability-ROIs were classified as "provincial sociality-ROIs" and "provincial imageability-ROIs". The matrix presented the average RSFC between each pair of ROIs across subjects.

Therefore, the dissociation between the brain regions showing sociality and imageability effects can only be partially explained by their intrinsic functional connectivity differences.

In the second set of comparisons, we investigated whether the dissociation between the adjacent connector ROIs (i.e., ROIs in the AG/MTG and PC/precuneus) of different groups is related

to their intrinsic functional connectivity to the provincial ROIs (i.e., ROIs outside the AG/MTG and PC/precuneus). We found that the provincial sociality-ROIs showed stronger RSFC to connector sociality-ROIs than to connector imageability-ROIs (mean Fisher-transformed correlation [SD]: provincial sociality-ROIs to connector sociality-ROIs = 0.63 [0.20]; provincial sociality-ROIs to connector imageability-ROIs = 0.48 [0.18]; $t[16] = 5.36$, $P < 0.001$) and the provincial imageability-ROIs showed stronger RSFC to connector imageability-ROIs than to connector sociality-ROIs (mean Fisher-transformed correlation [SD]: provincial imageability-ROIs to connector imageability-ROIs = 0.41 [0.12]; provincial imageability-ROIs to connector sociality-ROIs = 0.31 [0.11]; $t[16] = 6.80$, $P < 0.001$). Therefore, the functional dissociation between the adjacent areas in the AG/MTG and PC/precuneus was associated with their intrinsic functional connectivity to the other regions of the 2 semantic subsystems.

Discussion

To explore the neural substrates that process and integrate social and sensory–motor semantic attributes, we investigated the brain activities associated with the sociality and imageability of verbs in an fMRI experiment. The effects of both factors and their interaction were observed within the multimodal cortical semantic network. In addition, conjunction of the 2 main effects was observed in the bilateral AG/MTG.

The sociality effect observed in the present study replicated the findings of our previous study (Lin et al. 2015): high-sociality verbs evoked stronger activation than low-sociality verbs in the PC/precuneus, AG/MTG/STG, DMPFC, and ASTS. This finding demonstrated that the observed sociality effect in word semantic processing is not a reflection of the confounding effect of imageability. In addition, the social and private action verbs used in Lin et al. (2015) largely corresponded to the high-sociality verbs used in the present study, all of which refer to human physical actions. The present study further indicated that a similar sociality effect on brain activation also exists in the processing of low-imageability verbs, which mainly refer to mental events.

The imageability effects observed in the present study replicated the findings of previous studies using nouns as stimuli (Jessen et al. 2000; Binder et al. 2005; Sabsevitz et al. 2005; Fliessbach et al. 2006; Graves et al. 2010): high-imageability words evoked stronger activation than low-imageability words in the PC/precuneus, AG/MOG/MTG, VMTC, and SFG/MFG. Therefore, these brain regions support not only the sensory–motor semantic information of nouns, but also that of verbs. These results indicated that the lack of consistent findings on the imageability effect in previous studies could have resulted from uncontrolled confounding factors (see also Vigliocco et al. 2014). Given that the observed imageability and sociality effects partially overlapped each other, we propose that the sociality should be carefully controlled when investigating the imageability effect.

We conducted 3 follow-up analyses to explore the network properties of the brain regions showing sociality and imageability effects. In the first analysis, we found that the brain regions showing sociality effect highly overlap with the classic ToM network. This finding confirmed our hypothesis that the ToM network supports the processing of social semantic information of verbs (Lin et al. 2015) and is consistent with the view that the ToM network is a subsystem of the semantic network (Caramazza and Mahon 2006; Binder et al. 2016; Huth et al. 2016).

In the second analysis, we found that the brain regions showing sociality effect and those showing imageability effect were both mainly distributed in the default-mode network. This finding is consistent with the view that the default-mode network plays an important role in semantic processing (Binder et al. 2009). The dissociation of the 2 groups of brain regions does not follow the divides of the 7 intrinsic large-scale brain networks reported by Yeo et al. (2011) and thus cannot be attributed to the functional differences between them.

In the third analysis, we conducted ROI-based RSFC analysis to further explore the intrinsic functional connectivity properties of the brain regions showing sociality and imageability effects. The 2 groups of brain regions showed distinct RSFC characteristics: all sociality clusters had strong connectivity to each other; however, the imageability clusters connected with each other mainly through the AG/MTG and PC/precuneus and through the connectivity between the bihemispherically symmetric regions. We also found that the dissociation between the adjacent sociality and imageability clusters in the AG/MTG and PC/precuneus can be explained by their RSFC to the other sociality and imageability clusters. This finding was consistent with the view that the functions of a brain region depend in part on its intrinsic functional connectivity to the other brain regions (Mahon et al. 2007; Cole et al. 2016).

Our results have also revealed 2 types of connectors between these 2 subnetworks, with one type showing conjunction of the sociality and imageability effects and the other type showing interaction of the 2 effects. We observed the conjunction effect in bilateral AG/MTG. This conjunction effect can be explained by the hypothesis that the semantic network contains hierarchical convergence zones to process different types of semantic information (Damasio 1989; Fernandino et al. 2016): the regions showing a single effect (sociality or imageability) may serve as relatively low-level convergence zones processing a particular type (social or sensory–motor) of semantic information, whereas the regions showing both effects may serve as high-level convergence zones, which process both types of semantic information.

The conjunction of sociality and imageability effects in bilateral AG also provides new insights into the question of whether the AG activation in semantic tasks reflects semantic or nonsemantic processes. Although accumulating evidence has suggested that the AG activation reflects the semantic contents of stimuli (Fairhall and Caramazza 2013; Fernandino et al. 2015, 2016a, 2016b; Huth et al. 2016), a recent study (Humphreys et al. 2015) provided evidence that the activation level of AG might be explained by RT and thus might reflect nonsemantic processes sensitive to task difficulty. Although the present and previous studies (Binder et al. 2005; Graves et al. 2010) have tried to remove the effect of RT in data analysis, it remains possible that the RT effect cannot be fully controlled by current modeling methods (Grinband et al. 2008). In our results, the directions of RT effects associated with the sociality and imageability effects were reversed: the average RT of the high-sociality trials was significantly longer than that of the low-sociality trials; the average RT of the high-imageability trials was significantly shorter than that of the low-imageability trials. Given that the 2 reverse directions of RT effects should never overlap with each other, the observed conjunction effect indicated that the AG activation during semantic processing cannot be fully explained by RT.

The interaction effect of sociality and imageability was observed in the left ASTS. Although the left ATL has been proposed to be important for semantic representation (Patterson et al. 2007) and integration (Bemis and Pylkkanen 2011; Zhang and Pylkkanen 2015), the specific role of the left ASTS in semantic processing remains unclear. In the present study, its activation level for the HSHI verbs was high and its activation

level for the other 3 types of verbs was low and approximately the same (Fig. 1C). In other words, its activation level was high only when both the social and sensory–motor semantic attributes were rich and were combined tightly in a single concept. Therefore, we propose that this region represents associations between social and sensory–motor semantic attributes but not these attributes per se.

Finally, our task activation results converge with the findings of a previous study based on RSFC analysis (Xu et al. 2016). Xu et al. (2016) dissociated the multimodal semantic network into 3 subnetworks based on the RSFC data. Two of these subnetworks largely correspond to brain regions showing social and sensory–motor effects in the present study. In addition, their analysis also implicated the AG and ASTS as connectors between the 2 subnetworks. Therefore, convergent findings from the present study provide important clues for the cognitive functions of the subnetworks and their connectors reported in Xu et al. (2016). However, it should be noted that the multimodal semantic network may process not only social and sensory–motor semantic information but also other types of semantic information. Therefore, the function of the brain regions observed in the present study may not be limited to processing social and sensory–motor semantics.

In conclusion, we found that the semantic network contains 2 subnetworks that process social and sensory–motor semantic information, respectively. These 2 subnetworks have overlaps in the bilateral AG/MTG (and perhaps in the PC/precuneus), which may serve as a high-level convergence zone to process both types of semantic information. The left ASTS showed interaction between social and sensory–motor semantics and may selectively represent associations between social and sensory–motor semantic attributes. Thus, our findings revealed fine subdivisions of the multimodal cortical semantic network to process and integrate social and sensory–motor semantic information.

Supplementary Material

Supplementary material is available at *Cerebral Cortex* online.

Funding

National Natural Science Foundation of China (Grant numbers: 31300842, 31500882, and 31571125) and Beijing Advanced Innovation Center for Imaging Technology (BAICIT-2016018).

Notes

We thank Ming Liu and Aiping Ni for their help in the preparation of experiment; and Xi Yu, Wei Shen, Xiaohong Yang, and Yanchao Bi for helpful discussions. *Conflict of Interest*: None declared.

References

Ashburner J, Friston KJ. 2005. Unified segmentation. Neuroimage. 26:839–851.

Azuma T, Van Orden GC. 1997. Why SAFE is better than FAST: the relatedness of a word's meanings affects lexical decision times. J Mem Lang. 36:484–504.

Bedny M, Thompson-Schill SL. 2006. Neuroanatomically separable effects of imageability and grammatical class during single-word comprehension. Brain Lang. 98:127–139.

Bemis DK, Pylkkanen L. 2011. Simple composition: a magnetoencephalography investigation into the comprehension of minimal linguistic phrases. J Neurosci. 31:2801–2814.

Binder JR, Conant LL, Humphries CJ, Fernandino L, Simons SB, Aguilar M, Desai RH. 2016. Toward a brain-based componential semantic representation. Cogn Neuropsychol. 33:130–174.

Binder JR, Desai RH, Graves WW, Conant LL. 2009. Where is the semantic system? A critical review and meta-analysis of 120 functional neuroimaging studies. Cereb Cortex. 19: 2767–2796.

Binder JR, Westbury CF, McKiernan KA, Possing ET, Medler DA. 2005. Distinct brain systems for processing concrete and abstract concepts. J Cogn Neurosci. 17:905–917.

Binney RJ, Hoffman P, Ralph MAL. 2016. Mapping the multiple graded contributions of the anterior temporal lobe representational hub to abstract and social concepts: evidence from distortion-corrected fMRI. Cereb Cortex. 26:4227–4241.

Caramazza A, Mahon BZ. 2006. The organisation of conceptual knowledge in the brain: the future's past and some future directions. Cogn Neuropsychol. 23:13–38.

Chinese Academy of Sciences. 2005. 现代汉语词典 (The contemporary Chinese dictionary). 6th ed. Beijing: The Commercial Press.

Cole MW, Ito T, Bassett DS, Schultz DH. 2016. Activity flow over resting-state networks shapes cognitive task activations. Nat Neurosci. 19:1718–1726.

Contreras JM, Banaji MR, Mitchell JP. 2012. Dissociable neural correlates of stereotypes and other forms of semantic knowledge. Soc Cogn Affect Neurosci. 7:764–770.

Damasio AR. 1989. Time-locked multiregional retroactivation: a systems-level proposal for the neural substrates of recall and recognition. Cognition. 33:25–62.

Dodell-Feder D, Koster-Hale J, Bedny M, Saxe R. 2011. fMRI item analysis in a theory of mind task. Neuroimage. 55:705–712.

Eklund A, Nichols TE, Knutsson H. 2016. Cluster failure: why fMRI inferences for spatial extent have inflated false-positive rates. Proc Natl Acad Sci USA. 113:7900–7905.

Fairhall SL, Caramazza A. 2013. Brain regions that represent amodal conceptual knowledge. J Neurosci. 33:10552–10558.

Fernandino L, Binder JR, Desai RH, Pendl SL, Humphries CJ, Gross WL, Conant LL, Seidenberg MS. 2016a. Concept representation reflects multimodal abstraction: a framework for embodied semantics. Cereb Cortex. 26:2018–2034.

Fernandino L, Humphries CJ, Conant LL, Seidenberg MS, Binder JR. 2016b. Heteromodal cortical areas encode sensory-motor features of word meaning. J Neurosci. 36:9763–9769.

Fernandino L, Humphries CJ, Seidenberg MS, Gross WL, Conant LL, Binder JR. 2015. Predicting brain activation patterns associated with individual lexical concepts based on five sensory-motor attributes. Neuropsychologia. 76:17–26.

Ferstl EC, Neumann J, Bogler C, von Cramon DY. 2008. The extended language network: a meta-analysis of neuroimaging studies on text comprehension. Hum Brain Mapp. 29: 581–593.

Fliessbach K, Weis S, Klaver P, Elger CE, Weber B. 2006. The effect of word concreteness on recognition memory. Neuroimage. 32:1413–1421.

Gallagher HL, Happe F, Brunswick N, Fletcher PC, Frith U, Frith CD. 2000. Reading the mind in cartoons and stories: an fMRI study of 'theory of mind' in verbal and nonverbal tasks. Neuropsychologia. 38:11–21.

Graves WW, Desai R, Humphries C, Seidenberg MS, Binder JR. 2010. Neural systems for reading aloud: a multiparametric approach. Cereb Cortex. 20:1799–1815.

Grinband J, Wager TD, Lindquist M, Ferrera VP, Hirsch J. 2008. Detection of time-varying signals in event-related fMRI designs. Neuroimage. 43:509–520.

Grossman M, Koenig P, DeVita C, Glosser G, Alsop D, Detre J, Gee J. 2002. Neural representation of verb meaning: an fMRI study. Hum Brain Mapp. 15:124–134.

Humphreys GF, Hoffman P, Visser M, Binney RJ, Ralph MAL. 2015. Establishing task- and modality-dependent dissociations between the semantic and default mode networks. Proc Natl Acad Sci USA. 112:7857–7862.

Hutchinson JB, Uncapher MR, Wagner AD. 2009. Posterior parietal cortex and episodic retrieval: convergent and divergent effects of attention and memory. Learn Mem. 16:343–356.

Hutchinson JB, Uncapher MR, Weiner KS, Bressler DW, Silver MA, Preston AR, Wagner AD. 2014. Functional heterogeneity in posterior parietal cortex across attention and episodic memory retrieval. Cereb Cortex. 24:49–66.

Huth AG, de Heer WA, Griffiths TL, Theunissen FE, Gallant JL. 2016. Natural speech reveals the semantic maps that tile human cerebral cortex. Nature. 532:453–458.

Jessen F, Heun R, Erb M, Granath DO, Klose U, Papassotiropoulos A, Grodd W. 2000. The concreteness effect: evidence for dual coding and context availability. Brain Lang. 74:103–112.

Lin N, Bi YC, Zhao Y, Luo CM, Li XS. 2015. The theory-of-mind network in support of action verb comprehension: evidence from an fMRI study. Brain Lang. 141:1–10.

Mahon BZ, Milleville SC, Negri GAL, Rumiati RI, Caramazza A, Martin A. 2007. Action-related properties shape object representations in the ventral stream. Neuron. 55:507–520.

Mar RA. 2011. The neural bases of social cognition and story comprehension. Annu Rev Psychol. 62:103–134.

Mars RB, Jbabdi S, Sallet J, O'Reilly JX, Croxson PL, Olivier E, Noonan MP, Bergmann C, Mitchell AS, Baxter MG, et al. 2011. Diffusion-weighted imaging tractography-based parcellation of the human parietal cortex and comparison with human and macaque resting-state functional connectivity. J Neurosci. 31:4087–4100.

Martin A, Haxby JV, Lalonde FM, Wiggs CL, Ungerleider LG. 1995. Discrete cortical regions associated with knowledge of color and knowledge of action. Science. 270:102–105.

Millis ML, Button SB. 1989. The effect of polysemy on lexical decision time: now you see it, how you don't. Mem Cognit. 17:141–147.

Mitchell JP, Heatherton TF, Macrae CN. 2002. Distinct neural systems subserve person and object knowledge. Proc Natl Acad Sci USA. 99:15238–15243.

Nelson SM, McDermott KB, Petersen SE. 2012. In favor of a 'fractionation' view of ventral parietal cortex: comment on Cabeza et al. Trends Cogn Sci. 16:399–400.

Nichols T, Brett M, Andersson J, Wager T, Poline JB. 2005. Valid conjunction inference with the minimum statistic. Neuroimage. 25:653–660.

Patterson K, Nestor PJ, Rogers TT. 2007. Where do you know what you know? The representation of semantic knowledge in the human brain. Nat Rev Neurosci. 8:976–987.

Perani D, Cappa SF, Schnur T, Tettamanti M, Collina S, Rosa MM, Fazio F. 1999. The neural correlates of verb and noun processing—a PET study. Brain. 122:2337–2344.

Pexman PM, Hargreaves IS, Edwards JD, Henry LC, Goodyear BG. 2007. Neural correlates of concreteness in semantic categorization. J Cogn Neurosci. 19:1407–1419.

Raposo A, Moss HE, Stamatakis EA, Tyler LK. 2009. Modulation of motor and premotor cortices by actions, action words and action sentences. Neuropsychologia. 47:388–396.

Rodd J, Gaskell G, Marslen-Wilson W. 2002. Making sense of semantic ambiguity: semantic competition in lexical access. J Mem Lang. 46:245–266.

Rodriguez-Ferreiro J, Gennari SP, Davies R, Cuetos F. 2011. Neural correlates of abstract verb processing. J Cogn Neurosci. 23:106–118.

Sabsevitz DS, Medler DA, Seidenberg M, Binder JR. 2005. Modulation of the semantic system by word imageability. Neuroimage. 27:188–200.

Schurz M, Radua J, Aichhorn M, Richlan F, Perner J. 2014. Fractionating theory of mind: a meta-analysis of functional brain imaging studies. Neurosci Biobehav Rev. 42:9–34.

Shen W, Li X. 2016. Processing and representation of ambiguous words in Chinese reading: evidence from eye movements. Front Psychol. 7:1713.

Shrout PE, Fleiss JL. 1979. Intraclass correlations: uses in assessing rater reliability. Psychol Bull. 86:420–428.

Song XW, Dong ZY, Long XY, Li SF, Zuo XN, Zhu CZ, He Y, Yan CG, Zang YF. 2011. REST: a toolkit for resting-state functional magnetic resonance imaging data processing. Plos One. 6:e25031.

Spreng RN, Mar RA, Kim ASN. 2009. The common neural basis of autobiographical memory, prospection, navigation, theory of mind, and the default mode: a quantitative meta-analysis. J Cogn Neurosci. 21:489–510.

Spunt RP, Kemmerer D, Adolphs R. 2016. The neural basis of conceptualizing the same action at different levels of abstraction. Soc Cogn Affect Neurosci. 11:1141–1151.

Saxe R, Kanwisher N. 2003. People thinking about thinking people: the role of the temporo-parietal junction in "theory of mind". Neuroimage. 19:1835–1842.

Silver N, Dunlap W. 1987. Averaging correlation coefficients: should Fisher's z-transformation be used? J Appl Psychol. 72:1979–1981.

Sun HL, Huang JP, Sun DJ, Li DJ, Xing HB. 1997. Introduction to language corpus system of modern Chinese study. Beijing: Peking University Publisher.

Tettamanti M, Buccino G, Saccuman MC, Gallese V, Danna M, Scifo P, Fazio F, Rizzolatti G, Cappa SF, Perani D. 2005. Listening to action-related sentences activates fronto-parietal motor circuits. J Cogn Neurosci. 17:273–281.

Tzourio-Mazoyer N, Landeau B, Papathanassiou D, Crivello F, Etard O, Delcroix N, Mazoyer B, Joliot M. 2002. Automated anatomical labeling of activations in SPM using a macroscopic anatomical parcellation of the MNI MRI single-subject brain. Neuroimage. 15:273–289.

Uddin LQ, Supekar K, Amin H, Rykhlevskaia E, Nguyen DA, Greicius MD, Menon V. 2010. Dissociable connectivity within human angular gyrus and intraparietal sulcus: evidence from functional and structural connectivity. Cereb Cortex. 20:2636–2646.

van Dam WO, Rueschemeyer SA, Bekkering H. 2010. How specifically are action verbs represented in the neural motor system: an fMRI study. Neuroimage. 53:1318–1325.

Vigliocco G, Kousta ST, Della Rosa PA, Vinson DP, Tettamanti M, Devlin JT, Cappa SF. 2014. The neural representation of abstract words: the role of emotion. Cereb Cortex. 24: 1767–1777.

Wang J, Conder JA, Blitzer DN, Shinkareva SV. 2010. Neural representation of abstract and concrete concepts: a meta-analysis of neuroimaging studies. Hum Brain Mapp. 31: 1459–1468.

Xia MR, Wang JH, He Y. 2013. BrainNet Viewer: a network visualization tool for human brain connectomics. Plos One. 8:e68910.

Xu YW, Lin QX, Han ZZ, He Y, Bi YC. 2016. Intrinsic functional network architecture of human semantic processing: modules and hubs. Neuroimage. 132:542–555.

Yan CG, Wang XD, Zuo XN, Zang YF. 2016. DPABI: data processing & analysis for (resting-state) brain imaging. Neuroinformatics. 14:339–351.

Yan CG, Zang YF. 2010. DPARSF: a MATLAB toolbox for "pipeline" data analysis of resting-state fMRI. Front Syst Neurosci. 4:13.

Yarkoni T, Barch DM, Gray JR, Conturo TE, Braver TS. 2009. BOLD correlates of trial-by-trial reaction time variability in gray and white matter: a multi-study fMRI analysis. Plos One. 4:e4257.

Yeo BTT, Krienen FM, Sepulcre J, Sabuncu MR, Lashkari D, Hollinshead M, Roffman JL, Smoller JW, Zoller L, Polimeni JR, et al. 2011. The organization of the human cerebral cortex estimated by intrinsic functional connectivity. J Neurophysiol. 106:1125–1165.

Zahn R, Moll J, Krueger F, Huey ED, Garrido G, Grafman J. 2007. Social concepts are represented in the superior anterior temporal cortex. Proc Natl Acad Sci USA. 104:6430–6435.

Zhang LM, Pylkkanen L. 2015. The interplay of composition and concept specificity in the left anterior temporal lobe: an MEG study. Neuroimage. 111:228–240.